Supplementary Information

Theoretical and experimental analysis links isoform-specific ERK signalling to cell fate decisions

Marcel Schilling, Thomas Maiwald, Stefan Hengl, Dominic Winter, Clemens Kreutz, Walter Kolch, Wolf D. Lehmann, Jens Timmer, and Ursula Klingmüller

Supplementary Tables

Supplementary Table 1: Relative molar abundances of the non-, mono-, and double-phosphorylated peptide species derived from ERK1 and ERK2 before and after stimulation by Epo determined by UPLC-ESI-MS. The MS ion abundances were converted to relative molar concentrations as described in the text. N.d., not detectable.

peptide	rel. abundance (%) before stimulation	peptide	rel. abundance (%) after stimulation
IADPE-TEY-	100	IADPE-TEY-	63
IADPE-TEpY-	n.d.	IADPE-TEpY-	25
IADPE-pTEpY-	n.d.	IADPE-pTEpY-	12
VADPD-TEY-	97.7	VADPD-TEY-	51
VADPD-TEpY-	2	VADPD-TEpY-	29
VADPD-pTEpY-	0.3	VADPD-pTEpY-	20

Supplementary Table 2: Analysis of additional negative and positive feedback in the model. The nested models were compared to the original model using a likelihood-ratio test.

Model	χ^2	#parameters	p(LRT)
Original	186.569	32	
ppMEK → MEK by ppERK	182.190	36	0.3571
pRaf → Raf by ppERK	185.981	34	0.7453
pRaf → Raf by ppMEK	185.693	34	0.6456
MEK → ppMEK by ppERK	183.342	36	0.5206
Raf → pRaf by ppERK	185.868	34	0.7043
Raf → pRaf by ppMEK	185.940	34	0.7302

Supplementary figure legends

Supplementary Figure 1 Ordinary differential equations, parameters, observables, scaling factors and constraints for the mathematical model. Ordinary differential equations (ODE) are shown for the mathematical model of the Epo-induced ERK signalling pathway. Delayed activation of membrane-associated SHP1 was modelled using the linear chain trick approach realised with a 9-step compartmentalisation reaction. Parameters, observables, scaling factors, and constraints are shown with the respective descriptions.

Supplementary Figure 2 Quantitative immunoblotting data of primary erythroid progenitor cells stimulated with erythropoietin. Primary erythroid progenitor cells of the colony-forming unit erythroid stage (CFU-E) were stimulated with 50 U/ml Epo and samples were taken up to 70 min after adding Epo. Cellular lysates were either first subjected to immunoprecipitation (IP) or separated directly (TCL) in a randomised order by SDS-PAGE followed by quantitative immunoblotting (IB). GST-JAK2 and GST-EpoR were added prior to IP acting as calibrators. These calibrators as well as the normalisers β-actin and Clathrin HC were used to normalise the data.

Supplementary Figure 3 The polyclonal antibodies used in this study do not cross-react with single-phosphorylated MEK/ERK in a way that would have a significant influence on the results. (**A**) Primary CFU-E cells were stimulated for five different times with 50 U/ml Epo and the cellular lysates were loaded on two gels in triplicates. The first blot was analysed with the polyclonal antibodies that were used in the study, the second blot with monoclonal antibodies that specifically only recognise the double-phosphorylated MEK or the double-phosphorylated ERK. (**B**) Quantification of the results shows that both types of antibodies result in comparable dynamics of double-phosphorylated MEK2 and double-phosphorylated ERK2. (**C**) A strong and linear correlation of the results obtained with the polyclonal antibodies and the monoclonal antibodies is depicted for double-phosphorylated MEK2 and double-phosphorylated ERK2.

Supplementary Figure 4 Model selection for the plasma membrane module. (**A**) *Dynamic complex model*: EpoR and JAK2 are modelled being in rapid equilibrium. Gray shading indicates components of biological complexes that were not directly represented in the model Deactivation is modelled by a delayed activation of SHP1. (**B**) *Stable complex model*: EpoR

and JAK2 are modelled as a stable complex. Deactivation is modelled by a desensitation step. (**C**) *Stable complex and subcompartment model*: EpoR and JAK2 are modelled as a stable complex. Deactivation is modelled by a desensitation step with a subcompartment of a desensitised, dephosphorylated complex. Process diagram and fits to experimental data are shown. Green shading indicates variables contributing to the observed pJAK2, red shading depicts variables contributing to the observed pEpoR and yellow shading indicates contributions to both.

Supplementary Figure 5 The dose response of phosphorylated JAK2 and EpoR versus Epo is sigmoidal and can be explained by the *dynamic complex model*. (**A**) CFU-E cells were stimulated for 7 min with Epo concentrations ranging from 0.1 to 1000 U/ml and the phosphorylated and total amount of JAK2 and EpoR were analysed by quantitative immunoblotting. (**B**) The immunoblots shown in (A) were quantified and computationally processed. Error bars indicate standard deviations of three biological replicates. (**C**) Dose response profiles of phosphorylated JAK2 at 7 min were simulated using the *stable complex and subcompartment model* (see Figure 4C) and the *dynamic complex model* (see Figure 4A). Predicted values were scaled to the experimental data.

Supplementary Figure 6 Saturation of the kinases does not explain the observed signalling behaviour and modeling complex formation leads to over-parametrisation. (**A**) Two additional models (complex processive model and complex distributive model) were created by adding complex formation to the phosphorylation reactions of MEK and ERK. (**B**) Parameters for the models were estimated (1000 fits with quasi-random start values) and the best fit of each model is depicted (dashed lines). Experimental data are depicted as open circles with error bars indicating standard deviations estimated with a smoothing spline approach as described in materials and methods - mathematical modelling, parameter estimation and simulations. (**C**) The complex distributive model displays the lowest χ^2 value, but a log-likelihood ratio test rejects this model compared to the original model (distributive model). The Akaike information criterion (AIC) ranks the distributive model as best.

Supplementary Figure 7 MAP-kinase activation mechanism is distributive for ERK and processive for MEK. (**A**) The reaction mechanism for the processive MAP-kinase activation model is shown. Parameter estimation was performed 1000 times with randomly generated starting values. (**B**) The reaction mechanism for the distributive MAP-kinase activation model

is shown. Parameter estimation was performed 1000 times with randomly generated starting values. The processive and the distributive model were compared with a log-likelihood ratio test, rejecting the processive model (p-value < 10^{-6}).

Supplementary Figure 8 MS/MS spectra of synthetic ERK phosphopeptides. (**A**) The MS/MS spectra of three synthetic ERK phosphopeptides and sequence information covering the phosphorylated region are depicted. (**B**) Reporter fragments for the pT-containing peptides are shown with the neutral loss of phosphoric acid.

Supplementary Figure 9 Label-free quantification of ERK phosphorylation. (**A**) Reporter fragments showing the pY immonium ion are depicted for the pY-containing synthetic ERK peptides. (**B**) UPLC-MS elution order of 4 synthetic analogues of the tryptic ERK2 peptides. The selected ion traces correspond to the $[M+3H]^{3+}$ ions of the peptides as indicated (m/z 715.3 for -TEY-; m/z 742.0 for -TEpY- and -pTEY-; m/z 768.6 for -pTEpY-). (**C**) Correction factors for conversion of the measured relative ion intensities of the tryptic ERK2 peptide VADPDHDHTGFLTEYVATR into relative molar abundances. The experimental ion intensity values are divided by the given correction factor for conversion into relative molar abundances.

Supplementary Figure 10 Iterative rounds of parameter estimation and identifiability testing result in accurate determination of identifiable parameters. Parameters, initial concentrations, and scaling factors are displayed in red for standard deviations larger than 15% and in green for standard deviations equal to or smaller than 15%. For each iterative round, 1000 fits were performed and the mean values and standard deviation of each parameter was calculated on the basis of the best 50% of fits. Non-parametric bootstrap-based identifiability testing with the mean optimal transformation approach (MOTA) revealed dependent parameter doublets, triplets, or quadruplets, indicated by upper case letters (A – F). Dependent parameters were fixed to the value of the best fit and parameter estimation was performed again. After restraining the parameter space to 21 parameters, all parameters could be identified.

Supplementary Figure 11 Parameter doublets, triplets, and quadruplets analytically dependent as identified with the mean optimal transformation approach (MOTA). Analytically dependent parameters identified by MOTA are shown, with upper case letters corresponding to the dependent parameter doublets, triplets, or quadruplets in Supplementary

Figure 10. Data points (circles) represent the estimated parameter values of the best 500 fits of the specific parameter estimation round. The data points describe a straight line (**D**, **E**, **G**), a hyperbola (**A**, **F**, **I**), a two-dimensional surface (**B**, **C**), or a four-parameter dependency (**H**). In the first two cases (**A**, **D**, **E**, **F**, **G**, **I**), fixing one parameter identifies the second parameter; in the latter two cases (**B**, **C**, **H**), two parameters were fixed.

Supplementary Figure 12 Kinetics and signal amplification of the mathematical model. (**A**) Trajectories are depicted for all protein states of the dynamic pathway model. Data are shown for the observation period of 70 min after stimulation with Epo. mSHP1 and actSHP1 denotes membrane-localised and active SHP1, respectively. mSOS indicates membrane-localised SOS. (**B**) The time and the number of activated molecules at the maximum for pathway components are determined and signal amplification was calculated.

Supplementary Figure 13 Sensitivity analysis demonstrates that kinetic parameters control the amplitude of the Epo-induced ERK pathway. (**A**) Graphical representation of the quantities amplitude, integrated response, peak time, and duration. (**B**) Control coefficients of kinetic parameters for peak amplitude, integrated response, peak time, and signal duration of double-phosphorylated ERK1 and ERK2 are depicted. Positive control coefficients (shades of red) indicate higher values for the derived system quantities for increasing parameters, while negative control coefficients (shades of blue) indicate decreasing values for the quantities for increasing parameter values. Green fields represent no control. As expected by the summation theorems, the sum for parametric control coefficients equals 0 for peak amplitude and -1 for the other quantities.

Supplementary Figure 14 Overexpression of ERK1 and ERK2 increases differentiation in primary erythroid progenitor cells. Murine erythroid progenitor cells retrovirally transduced with ERK1, ERK2 or vector control were cultivated in serum-free medium supplemented with 0.5 U/ml Epo for the indicated time. Differentiation was measured by flow cytometry, scoring CD71-negative and Ter119-positive cells. Haemoglobin content was analyzed by flow cytometric staining against haemoglobin alpha. Enhanced differentiation as determined by the appearance of the surface marker Ter119 inversely correlates with reduced expression of haemoglobin alpha. It appears that reduction in cell proliferation and enhanced differentiation shortens the time window for transcription of the haemoglobin alpha gene before the cells eject the nucleus and therefore results in reduced haemoglobin expression.

Ordinary differential equations

JAK2: $\dot{x}_1 = -k_1 \cdot x_1 \cdot u1 + k_6 \cdot x_{10} \cdot x_{13}$

EpoR: $\dot{x}_2 = -k_2 \cdot x_2 \cdot x_{10} + k_5 \cdot x_{11} \cdot x_{13}$

SHP1: $\dot{x}_3 = -k_3 \cdot x_3 \cdot x_{11} + k_4 \cdot x_{13}$

SOS: $\dot{x}_4 = -k_7 \cdot x_4 \cdot x_{11} + k_8 \cdot x_{14} + k_{24} \cdot x_{20}$

Raf: $\dot{x}_5 = -k_9 \cdot x_5 \cdot x_{14} + k_{10} \cdot x_{15}$

MEK2: $\dot{x}_6 = -k_{11} \cdot x_6 \cdot x_{15} + k_{16} \cdot x_{21}$

MEK1: $\dot{x}_7 = -k_{13} \cdot x_7 \cdot x_{15} + k_{16} \cdot x_{22}$

ERK1: $\dot{x}_8 = -k_{17} \cdot x_8 \cdot x_{16} - k_{17} \cdot x_8 \cdot x_{17} + k_{22} \cdot x_{23}$

ERK2: $\dot{x}_9 = -k_{19} \cdot x_9 \cdot x_{16} - k_{19} \cdot x_9 \cdot x_{17} + k_{22} \cdot x_{24}$

pJAK2: $\dot{x}_{10} = +k_1 \cdot x_1 \cdot u1 - k_6 \cdot x_{10} \cdot x_{13}$

pEpoR: $\dot{x}_{11} = +k_2 \cdot x_2 \cdot x_{10} - k_5 \cdot x_{11} \cdot x_{13}$

mSHP1: $\dot{x}_{12} = +k_3 \cdot x_3 \cdot x_{11} - k_{3'} \cdot x_{12}$

actSHP1: $\dot{x}_{13} = +k_{3'} \cdot x_{32} - k_4 \cdot x_{13}$

mSOS: $\dot{x}_{14} = +k_7 \cdot x_4 \cdot x_{11} - k_8 \cdot x_{14} - k_{23} \cdot x_{14} \cdot x_{18} - k_{23} \cdot x_{14} \cdot x_{19}$

pRaf: $\dot{x}_{15} = +k_9 \cdot x_5 \cdot x_{14} - k_{10} \cdot x_{15}$

ppMEK2: $\dot{x}_{16} = +k_{12} \cdot x_{21} \cdot x_{15} - k_{15} \cdot x_{16}$

ppMEK1: $\dot{x}_{17} = +k_{14} \cdot x_{22} \cdot x_{15} - k_{15} \cdot x_{17}$

ppERK1: $\dot{x}_{18} = +k_{18} \cdot x_{23} \cdot x_{16} + k_{18} \cdot x_{23} \cdot x_{17} - k_{21} \cdot x_{18}$

ppERK2: $\dot{x}_{19} = +k_{20} \cdot x_{24} \cdot x_{16} + k_{20} \cdot x_{24} \cdot x_{17} - k_{21} \cdot x_{19}$

pSOS: $\dot{x}_{20} = +k_{23} \cdot x_{14} \cdot x_{18} + k_{23} \cdot x_{14} \cdot x_{19} - k_{24} \cdot x_{20}$

pMEK2: $\dot{x}_{21} = +k_{11} \cdot x_6 \cdot x_{15} - k_{12} \cdot x_{21} \cdot x_{15} + k_{15} \cdot x_{16} - k_{16} \cdot x_{21}$

pMEK1: $\dot{x}_{22} = +k_{13} \cdot x_7 \cdot x_{15} - k_{14} \cdot x_{22} \cdot x_{15} + k_{15} \cdot x_{17} - k_{16} \cdot x_{22}$

pERK1: $\dot{x}_{23} = +k_{17} \cdot x_8 \cdot x_{16} + k_{17} \cdot x_8 \cdot x_{17} - k_{18} \cdot x_{23} \cdot x_{16} - k_{18} \cdot x_{23} \cdot x_{17} + k_{21} \cdot x_{18} - k_{22} \cdot x_{23}$

pERK2: $\dot{x}_{24} = +k_{19} \cdot x_9 \cdot x_{16} + k_{19} \cdot x_9 \cdot x_{17} - k_{20} \cdot x_{24} \cdot x_{16} - k_{20} \cdot x_{24} \cdot x_{17} + k_{21} \cdot x_{19} - k_{22} \cdot x_{24}$

$mSHP1_{delay1}$: $\dot{x}_{25} = +k_{3'} \cdot x_{12} - k_{3'} \cdot x_{25}$

$mSHP1_{delay2}$: $\dot{x}_{26} = +k_{3'} \cdot x_{25} - k_{3'} \cdot x_{26}$

$mSHP1_{delay3}$: $\dot{x}_{27} = +k_{3'} \cdot x_{26} - k_{3'} \cdot x_{27}$

$mSHP1_{delay4}$: $\dot{x}_{28} = +k_{3'} \cdot x_{27} - k_{3'} \cdot x_{28}$

$mSHP1_{delay5}$: $\dot{x}_{29} = +k_{3'} \cdot x_{28} - k_{3'} \cdot x_{29}$

$mSHP1_{delay6}$: $\dot{x}_{30} = +k_{3'} \cdot x_{29} - k_{3'} \cdot x_{30}$

$mSHP1_{delay7}$: $\dot{x}_{31} = +k_{3'} \cdot x_{30} - k_{3'} \cdot x_{31}$

$mSHP1_{delay8}$: $\dot{x}_{32} = +k_{3'} \cdot x_{31} - k_{3'} \cdot x_{32}$

Parameters

JAK2 phosphorylation by Epo:	k_1
EpoR phosphorylation by pJAK2:	k_2
SHP1 activation by pEpoR:	k_3
SHP1 delay:	$k_{3'}$
actSHP1 deactivation:	k_4
pEpoR dephosphorylation by actSHP1:	k_5
pJAK2 dephosphorylation by actSHP1:	k_6
SOS recruitment by pEpoR:	k_7
mSOS release from membrane:	k_8
mSOS induced Raf phosphorylation:	k_9
pRaf dephosphorylation:	k_{10}
1st MEK2 phosphorylation by pRaf:	k_{11}
2nd MEK2 phosphorylation by pRaf:	k_{12}
1st MEK1 phosphorylation by pRaf:	k_{13}
2nd MEK1 phosphorylation by pRaf:	k_{14}
1st MEK dephosphorylation:	k_{15}
2nd MEK dephosphorylation:	k_{16}
1st ERK1 phosphorylation by ppMEK:	k_{17}
2nd ERK1 phosphorylation by ppMEK:	k_{18}
1st ERK2 phosphorylation by ppMEK:	k_{19}
2nd ERK2 phosphorylation by ppMEK:	k_{20}
1st ERK dephosphorylation:	k_{21}
2nd ERK dephosphorylation:	k_{22}
ppERK neg feedback on mSOS:	k_{23}
pSOS dephosphorylation:	k_{24}

Observables

pEpoR:	$y_1 = s_1 \cdot x_{11}$
pJAK2:	$y_2 = s_2 \cdot x_{10}$
ppMEK2:	$y_3 = s_3 \cdot x_{16}$
ppMEK1:	$y_4 = s_3 \cdot x_{17}$
ppERK1:	$y_5 = s_4 \cdot x_{18}$
ppERK2:	$y_6 = s_4 \cdot x_{19}$
pSOS:	$y_7 = s_5 \cdot x_{20}$
SOS + mSOS:	$y_8 = s_5 \cdot (x_4 + x_{14})$

Scaling factors

scale pEpoR:	s_1
scale pJAK2:	s_2
scale ppMEK:	s_3
scale ppERK:	s_4
scale SOS:	s_5

Constraints

$pERK1_{max} / ERK1_{max} = 0.2$

$pERK2_{max} / ERK2_{max} = 0.2$

$ppERK1_{max} / ERK1_{max} = 0.1$

$ppERK2_{max} / ERK2_{max} = 0.1$

Supplementary Figure 1, Schilling, Maiwald et al.

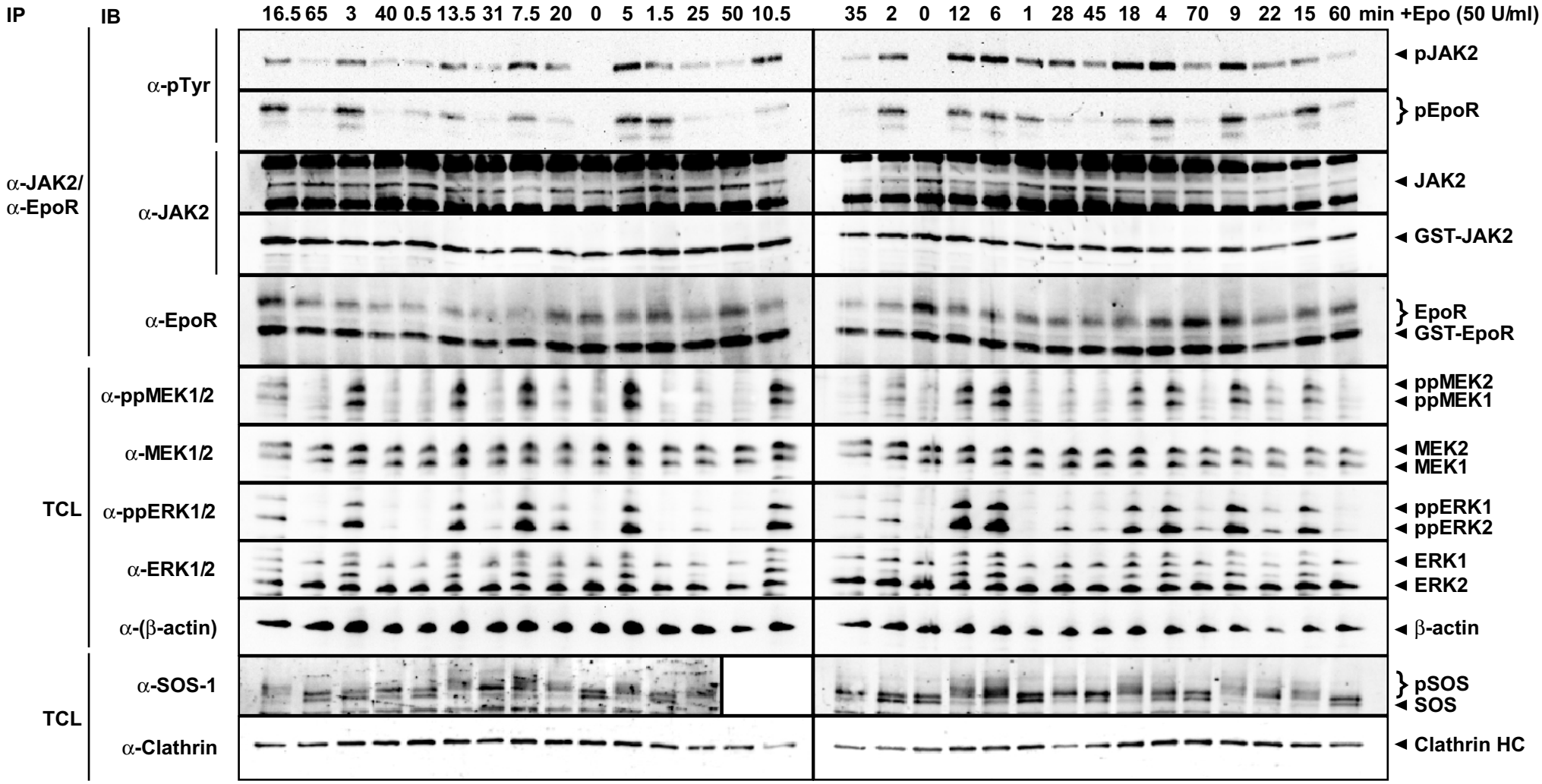

Supplementary Figure 2, Schilling, Maiwald et al.

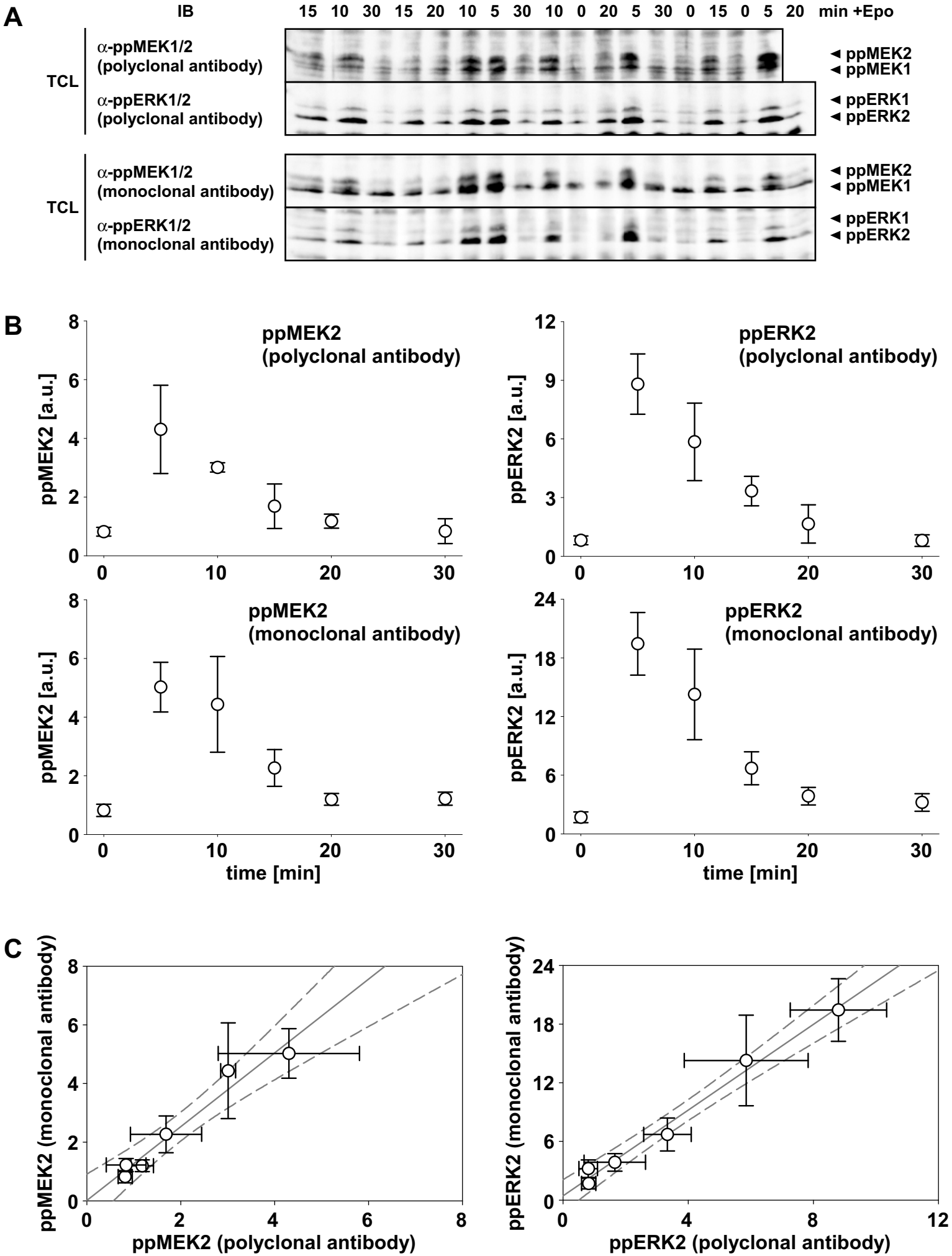

Supplementary Figure 3, Schilling, Maiwald et al.

A Dynamic complex model

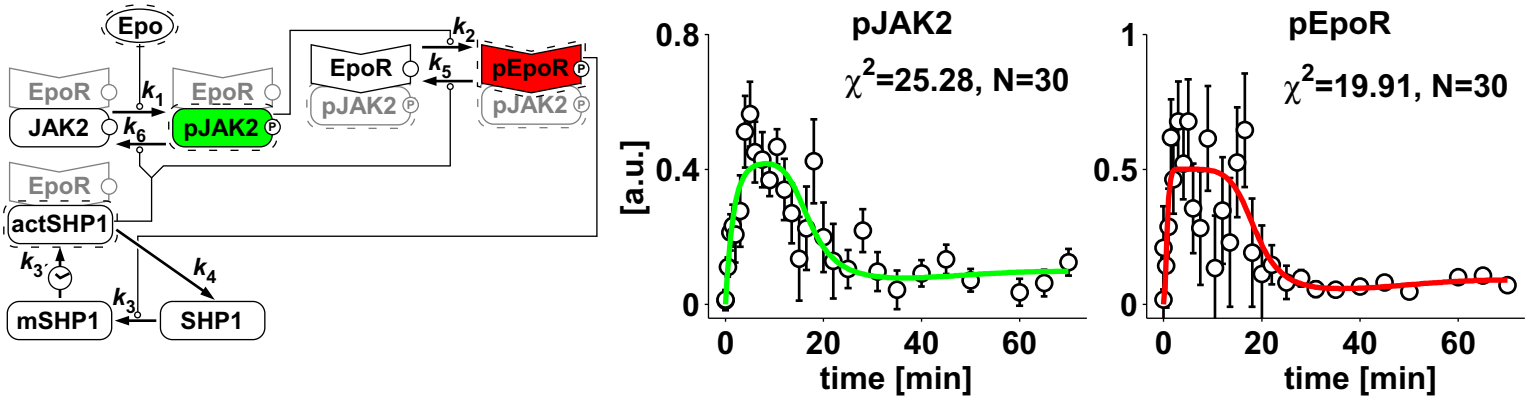

N=236; fitted parameters = 32; total χ^2 value = 181.3; AIC = 679.1

B Stable complex model

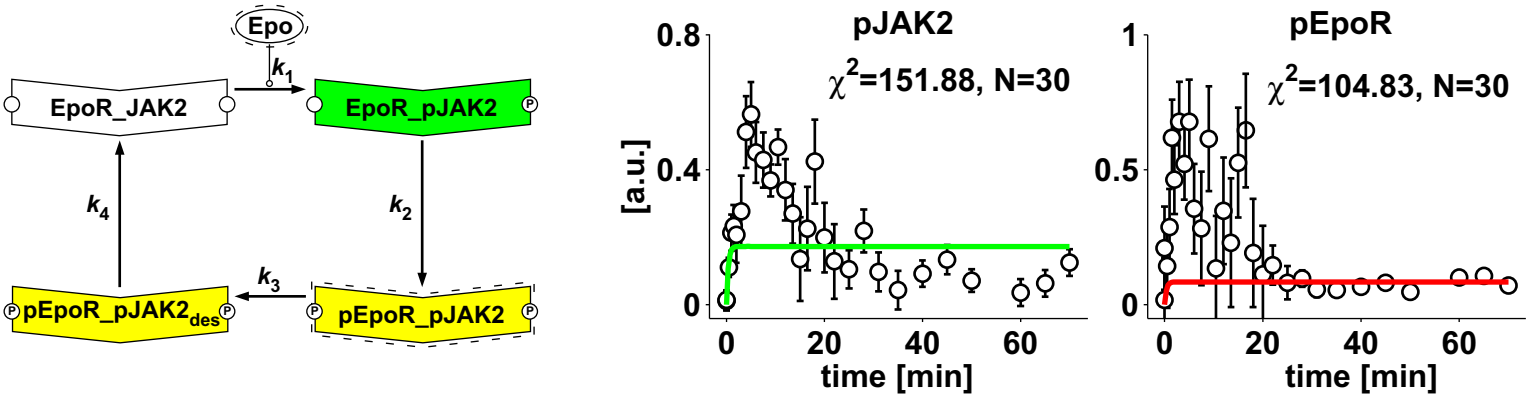

N=236; fitted parameters = 29; total χ^2 value = 392.5; AIC = 884.2

C Stable complex and subcompartment model

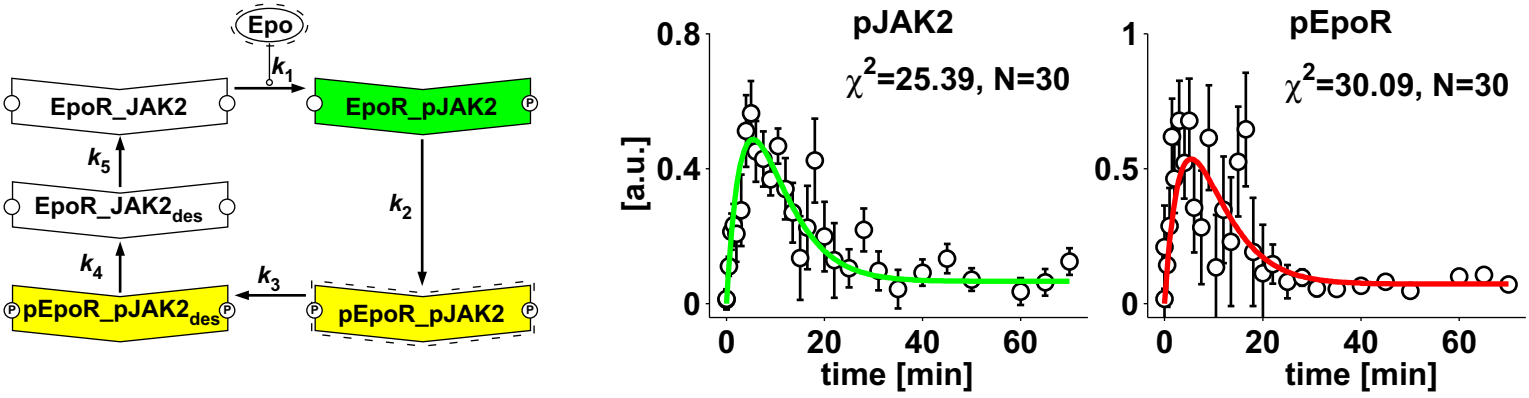

N=236; fitted parameters = 30; total χ^2 value = 191.4; AIC = 685.1

Supplementary Figure 4, Schilling, Maiwald et al.

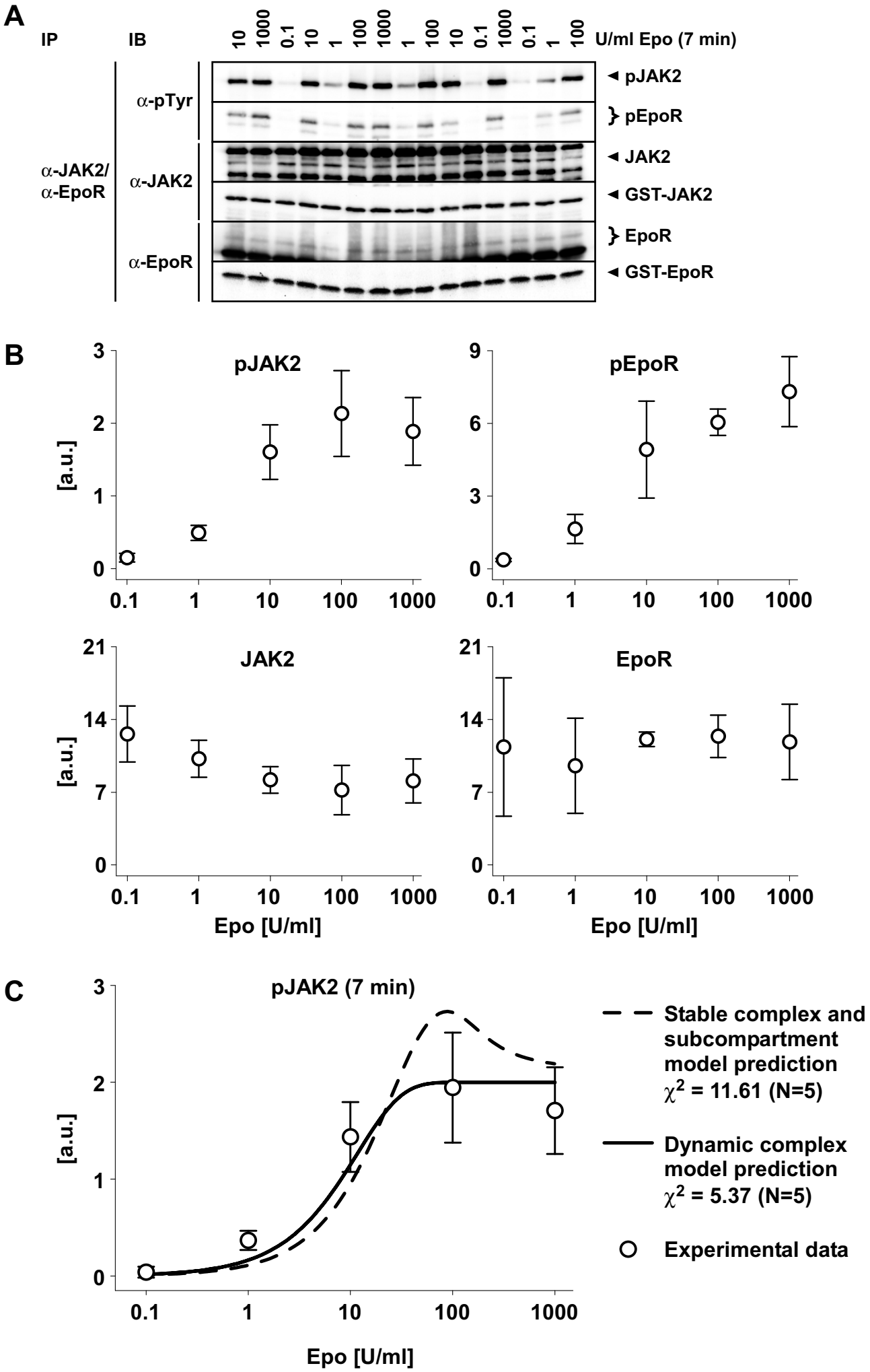

Supplementary Figure 5, Schilling, Maiwald et al.

A

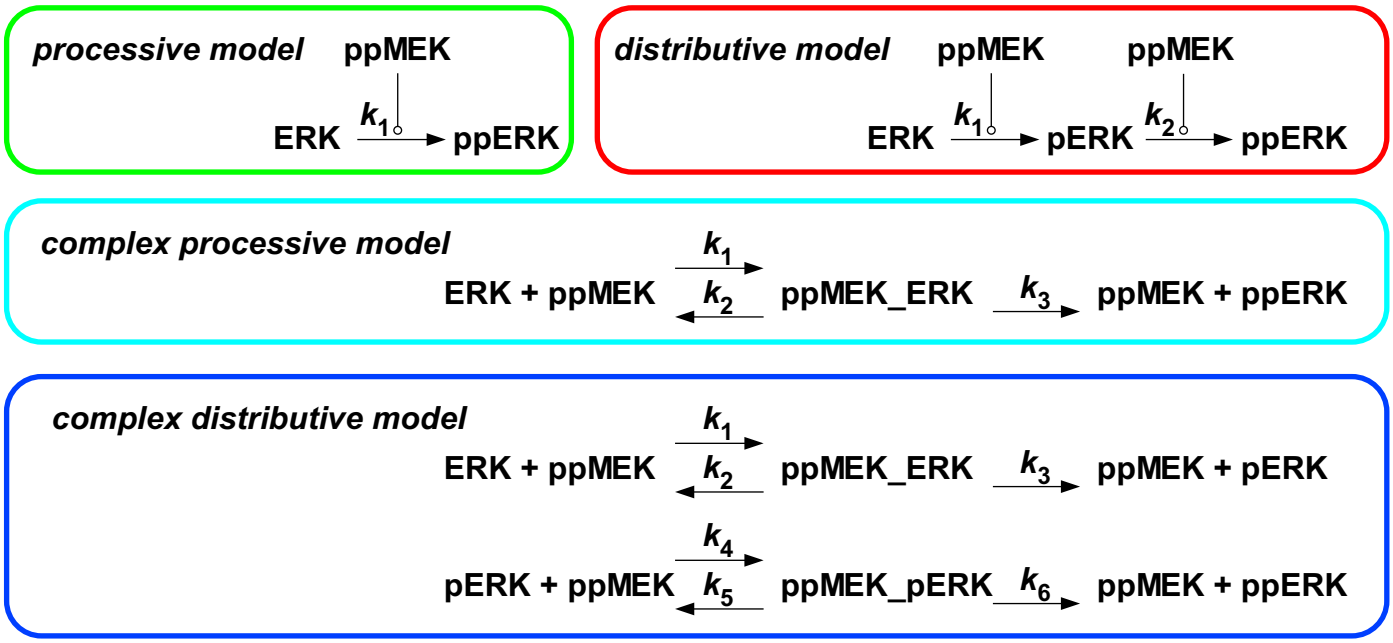

B

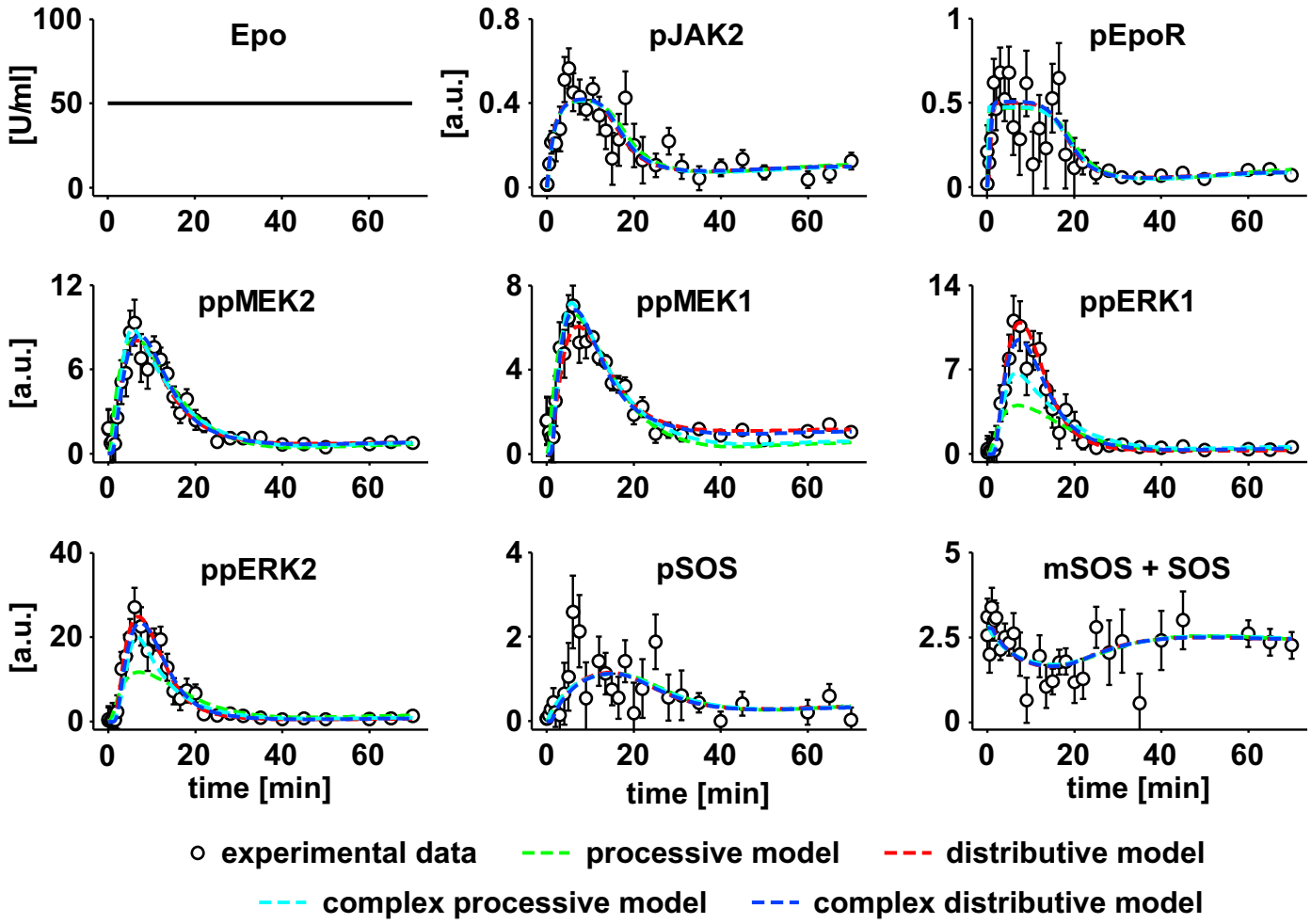

C

model	*fitted parameters*	*total χ^2 value*	*AIC*
processive model	26	390.8	878.7
distributive model	32	181.3	679.1
complex processive model	34	266.4	768.1
complex distributive model	48	173.6	703.4

Supplementary Figure 6, Schilling, Maiwald et al.

A **Processive MAP-kinase activation**

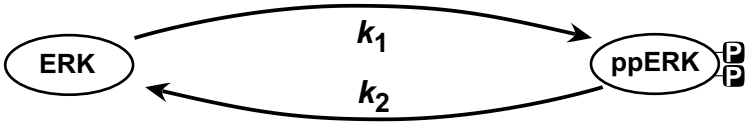

24 reactions
28 ODE
26 fitted parameters
236 data points
Total χ^2 value: 390.8
Akaike information criterion (AIC): 878.7

B **Distributive MAP-kinase activation**

34 reactions
32 ODE
32 fitted parameters
236 data points
Total χ^2 value: 181.3
Akaike information criterion (AIC): 679.1

Processive MEK activation	[$min^{-1}(10^4 molecules)^{-1}$]
1st MEK2 phosphorylation by pRaf	4.083
2nd MEK2 phosphorylation by pRaf	318.4
1st MEK1 phosphorylation by pRaf	0.9448
2nd MEK1 phosphorylation by pRaf	858.8

Distributive ERK activation	[$min^{-1}(10^4 molecules)^{-1}$]
1st ERK1 phosphorylation by ppMEK	2.825
2nd ERK1 phosphorylation by ppMEK	59.72
1st ERK2 phosphorylation by ppMEK	2.769
2nd ERK2 phosphorylation by ppMEK	53.23

Supplementary Figure 7, Schilling, Maiwald et al.

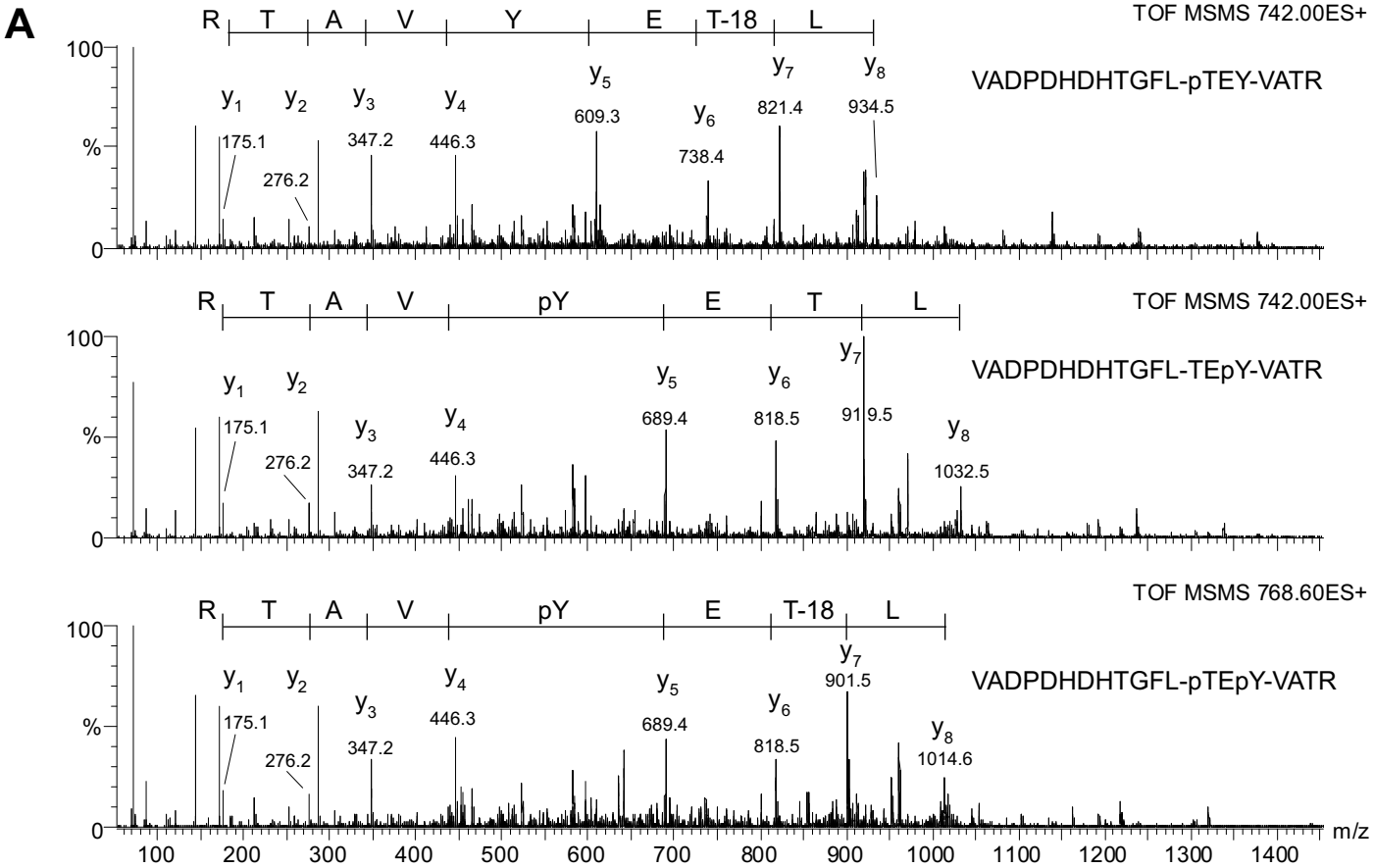

collision offset 34 V

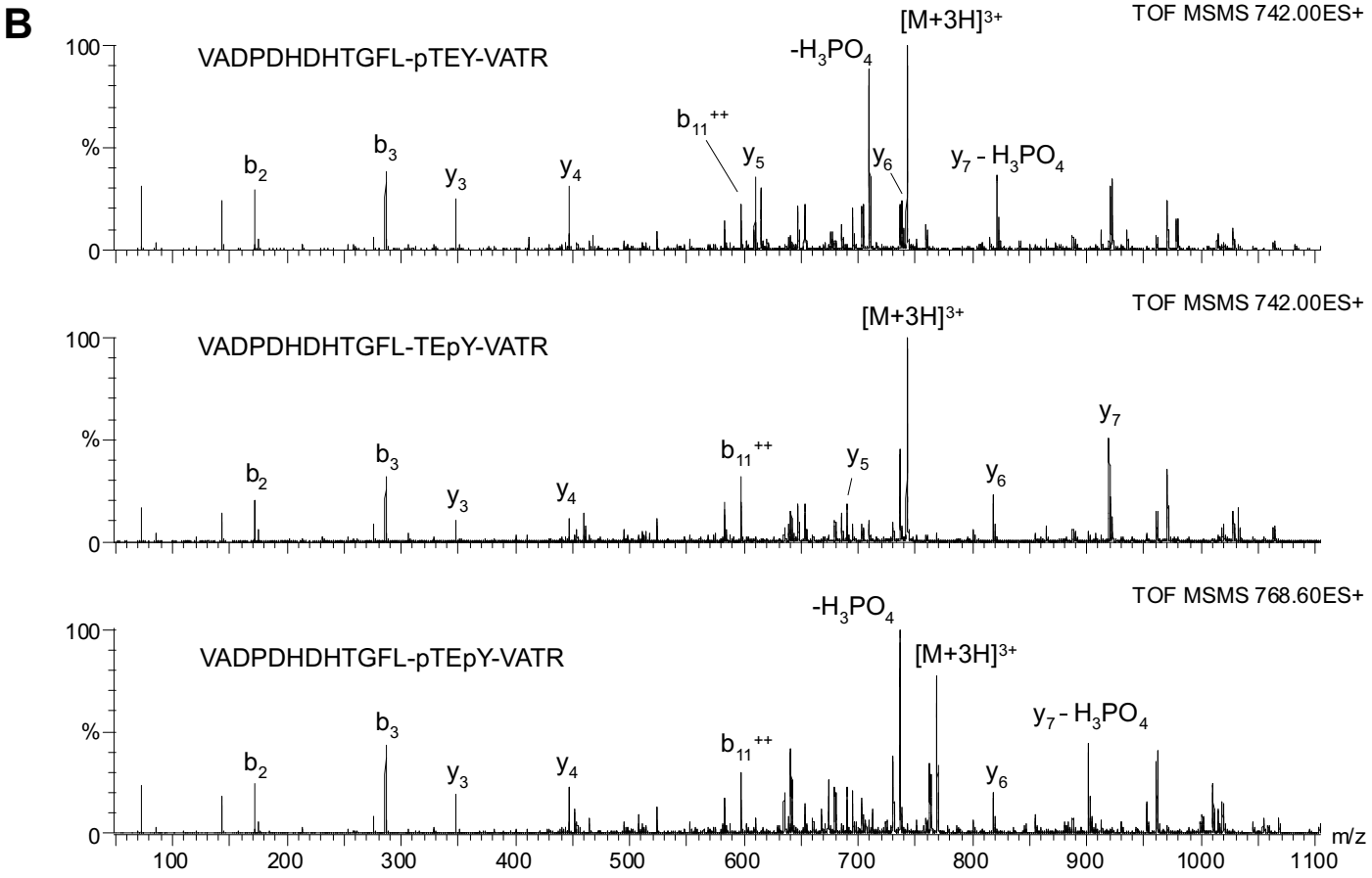

collision offset 28 V

Supplementary Figure 8, Schilling, Maiwald et al.

A

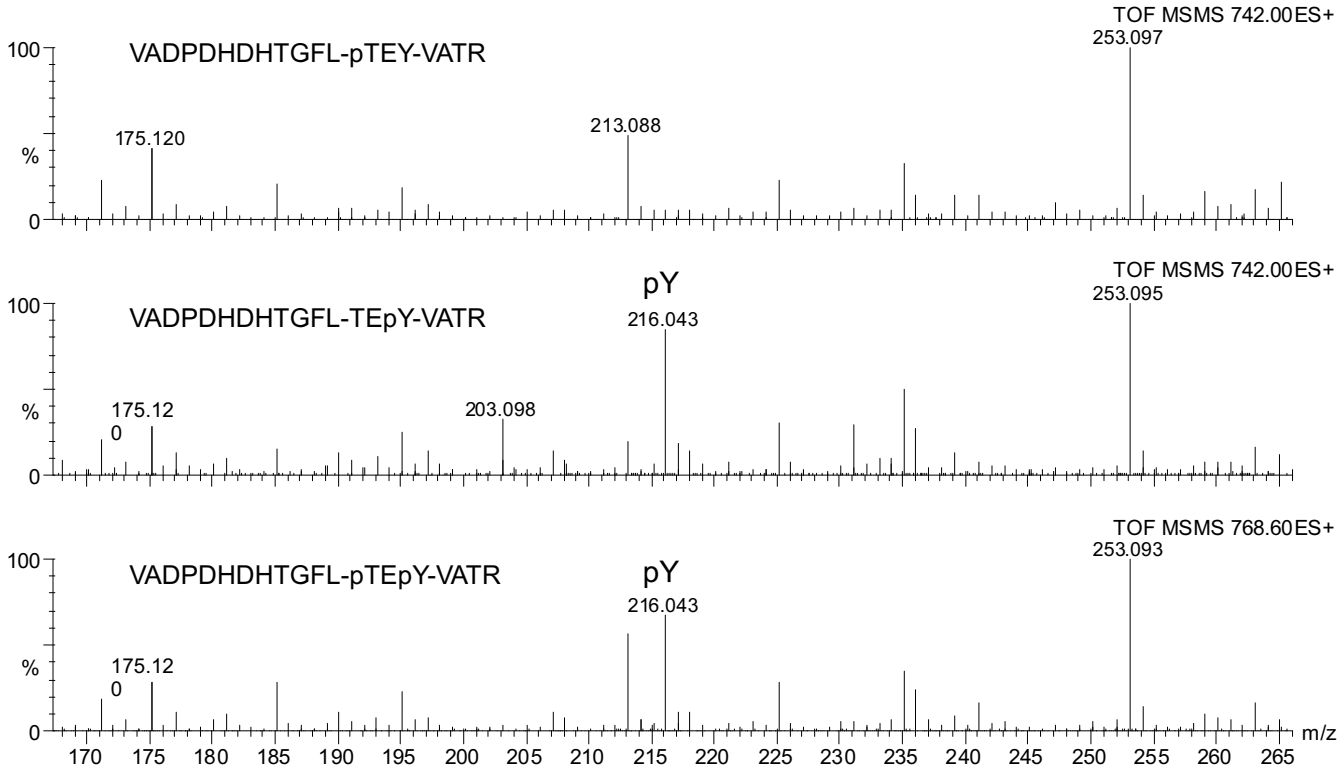

collision offset 50 V

B

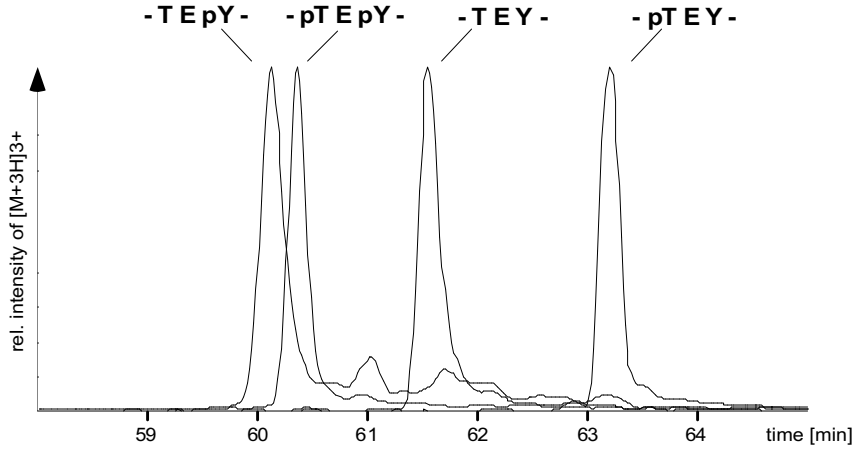

C

species	*rel. electrospray ionisation efficiency correction factor*	*rel. UPLC recovery correction factor*	*combined correction factor*
-TEY-	**1**	**1**	**1**
-TEpY-	**1.23**	**1.36**	**1.67**
-pTEpY-	**1.10**	**1.37**	**1.51**

Supplementary Figure 9, Schilling, Maiwald et al.

	32 parameters estimated	*MOTA*	*25 parameters estimated*	*MOTA*	*21 parameters estimated*	*Parameters*
JAK2 phosphorylation by Epo [$min^{-1}(U/ml)^{-1}$]	0.01229 ± 0.0002662 (2%)		0.01235 ± 0.000209 (2%)		0.01234 ± 0.0002096 (2%)	0.0122149
EpoR phosphorylation by pJAK2 [$min^{-1}(10^4 molecules)^{-1}$]	3.077 ± 0.5756 (19%)		2.968 ± 0.4354 (15%)	G	fixed	3.15714
SHP1 activation by pEpoR [$min^{-1}(10^4 molecules)^{-1}$]	0.4116 ± 0.008597 (2%)		0.4091 ± 0.002953 (1%)		0.4093 ± 0.003021 (1%)	0.408408
actSHP1 deactivation [$min^{-1}(10^4 molecules)^{-1}$]	0.02363 ± 0.001449 (6%)		0.0246 ± 0.000579 (2%)		0.0243 ± 0.0007702 (3%)	0.0248773
pEpoR dephosphorylation by actSHP1 [$min^{-1}(10^4 molecules)^{-1}$]	1.543 ± 1.157 (75%)		1.142 ± 0.162 (14%)	G	1.188 ± 0.02924 (2%)	1.19995
pJAK2 dephosphorylation by actSHP1 [$min^{-1}(10^4 molecules)^{-1}$]	0.4798 ± 0.3436 (72%)	A	0.3681 ± 0.00696 (2%)		0.3657 ± 0.00712 (2%)	0.368384
SOS recruitment by pEpoR[$min^{-1}(10^4 molecules)^{-1}$]	0.09929 ± 0.004602 (5%)		0.09869 ± 0.005082 (5%)		0.1025 ± 0.00847 (8%)	0.10271
mSOS release from membrane [min^{-1}]	11.54 ± 6.049 (52%)		11.34 ± 5.32 (47%)	H	15.43 ± 1.01 (7%)	15.5956
mSOS induced Raf phosphorylation[$min^{-1}(10^4 molecules)^{-1}$]	0.2005 ± 0.1733 (86%)		0.2029 ± 0.1447 (71%)	H	0.1453 ± 0.01783 (12%)	0.144515
pRaf dephosphorylation [min^{-1}]	0.3578 ± 0.01813 (5%)		0.3523 ± 0.01348 (4%)		0.3737 ± 0.003591 (1%)	0.374228
1st MEK2 phosphorylation by pRaf [$min^{-1}(10^4 molecules)^{-1}$]	4.083 ± 3.149 (77%)	B	2.884 ± 0.125 (4%)		3.118 ± 0.0313 (1%)	3.11919
2nd MEK2 phosphorylation by pRaf [$min^{-1}(10^4 molecules)^{-1}$]	318.4 ± 226.2 (71%)	C	fixed			215.158
1st MEK1 phosphorylation by pRaf [$min^{-1}(10^4 molecules)^{-1}$]	0.9448 ± 0.6336 (67%)	B	fixed			0.687193
2nd MEK1 phosphorylation by pRaf [$min^{-1}(10^4 molecules)^{-1}$]	858.8 ± 564.8 (66%)	C	597 ± 37.96 (6%)		665.5 ± 10.47 (2%)	667.957
1st MEK dephosphorylation [min^{-1}]	0.143 ± 0.009349 (7%)		0.1437 ± 0.008317 (6%)		0.1317 ± 0.001564 (1%)	0.130937
2nd MEK dephosphorylation [min^{-1}]	0.07794 ± 0.01871 (24%)	B, C	fixed			0.0732724
1st ERK1 phosphorylation by ppMEK [$min^{-1}(10^4 molecules)^{-1}$]	2.825 ± 2.035 (72%)	D	fixed			2.4927
2nd ERK1 phosphorylation by ppMEK [$min^{-1}(10^4 molecules)^{-1}$]	59.72 ± 41.84 (70%)	E	59.54 ± 0.1004 (0%)		59.56 ± 0.1582 (0%)	59.5251
1st ERK2 phosphorylation by ppMEK [$min^{-1}(10^4 molecules)^{-1}$]	2.769 ± 1.994 (72%)	D	2.443 ± 0.002752 (0%)		2.446 ± 0.003453	2.44361
2nd ERK2 phosphorylation by ppMEK [$min^{-1}(10^4 molecules)^{-1}$]	53.23 ± 37.31 (70%)	E	fixed		(0%)	53.081
1st ERK dephosphorylation [min^{-1}]	58.7 ± 40.72 (69%)		58.75 ± 13.46 (23%)	I	39.21 ± 0.1427 (0%)	39.0886
2nd ERK dephosphorylation [min^{-1}]	5.08 ± 3.407 (67%)		4.508 ± 1.027 (23%)	I	3.016 ± 0.007706 (0%)	3.00453
ppERK neg feedback on mSOS [$min^{-1}(10^4 molecules)^{-1}$]	5270 ± 2309 (44%)		5064 ± 2025 (40%)	H	fixed	5122.68
pSOS dephosphorylation [min^{-1}]	0.1216 ± 0.005523 (5%)		0.1211 ± 0.005964 (5%)		0.1255 ± 0.01053 (8%)	0.124944
JAK2 [$\times 10^4$molecules]	determined					2
EpoR [$\times 10^4$molecules]	determined					1
SHP1 [$\times 10^4$molecules]	13.09 ± 10.76 (82%)	A	fixed			10.7991
SOS [$\times 10^4$molecules]	3.107 ± 2.186 (70%)	F	2.51 ± 0.008011 (0%)		2.509 ± 0.01336 (1%)	2.5101
Raf [$\times 10^4$molecules]	5.201 ± 4.705 (90%)		5.138 ± 3.97 (77%)	H	fixed	3.7719
MEK2 [$\times 10^4$molecules]	determined					11
MEK1 [$\times 10^4$molecules]	determined					24
ERK1 [$\times 10^4$molecules]	determined					7
ERK2 [$\times 10^4$molecules]	determined					21
scale pEpoR [$\times 10^4$molecules/a.u.]	0.4964 ± 0.005524 (1%)		0.4968 ± 0.004462 (1%)		0.4926 ± 0.004916 (1%)	0.493312
scale pJAK2 [$\times 10^4$molecules/a.u.]	0.21 ± 0.001148 (1%)		0.2096 ± 0.000601 (0%)		0.2097 ± 0.0007172 (0%)	0.21008
scale ppMEK [$\times 10^4$molecules/a.u.]	28.37 ± 10.24 (36%)		28.13 ± 6.391 (23%)	I	fixed	40.5364
scale ppERK [$\times 10^4$molecules/a.u.]	13.44 ± 0.09748 (1%)		13.46 ± 0.1056 (1%)		13.64 ± 0.04152 (0%)	13.5981
scale SOS [$\times 10^4$molecules/a.u.]	1.379 ± 0.9862 (71%)	F	fixed			1.10228

Supplementary Figure 10, Schilling, Maiwald et al.

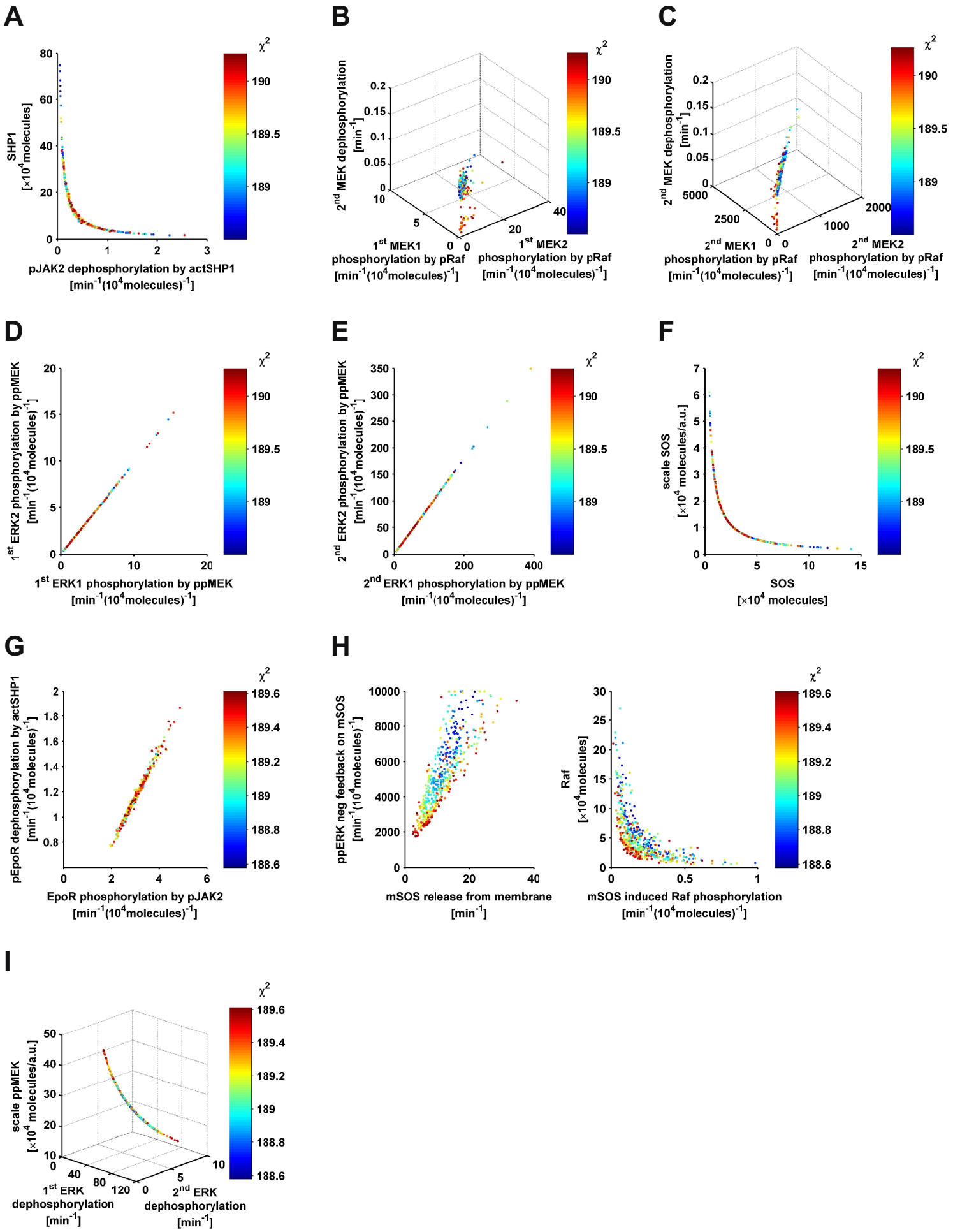

Supplementary Figure 11, Schilling, Maiwald et al.

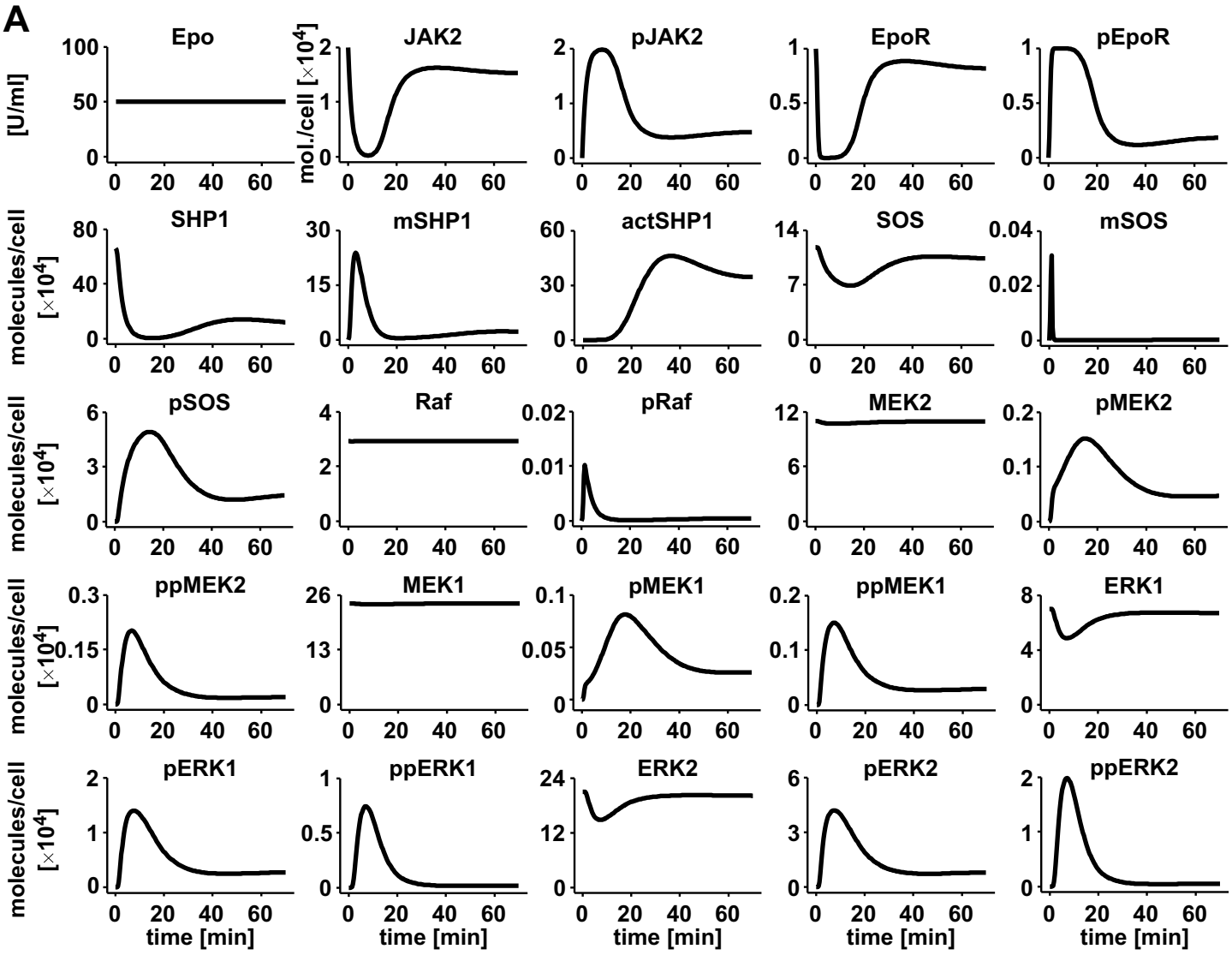

B

	JAK2	EpoR	SOS	Raf	MEK1/2	ERK1/2
time at maximum	8:27 min	3:52 min	1:03 min	1:24 min	6:51 min	7:02 min
total molecules	20000	10000	34100	54800	350000	280000
concentration	0.083 µM		0.142 µM	0.227 µM	1.453 µM	1.162 µM
activated molecules at maximum	19804	10000	130	57	5234	27272
signal amplification	×0.5	×0.013	×0.44	×92	×5	

Supplementary Figure 12, Schilling, Maiwald et al.

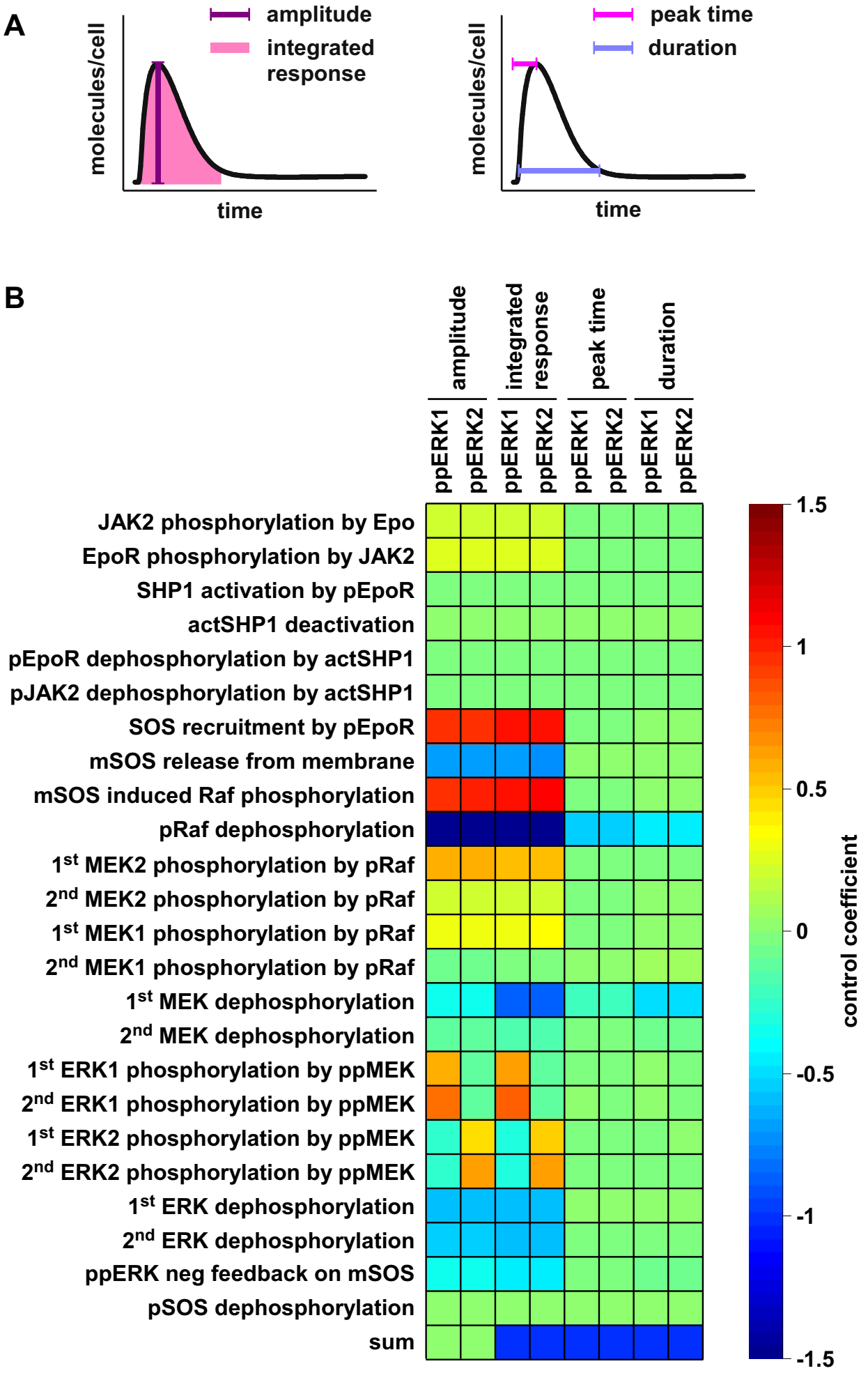

Supplementary Figure 13, Schilling, Maiwald et al.

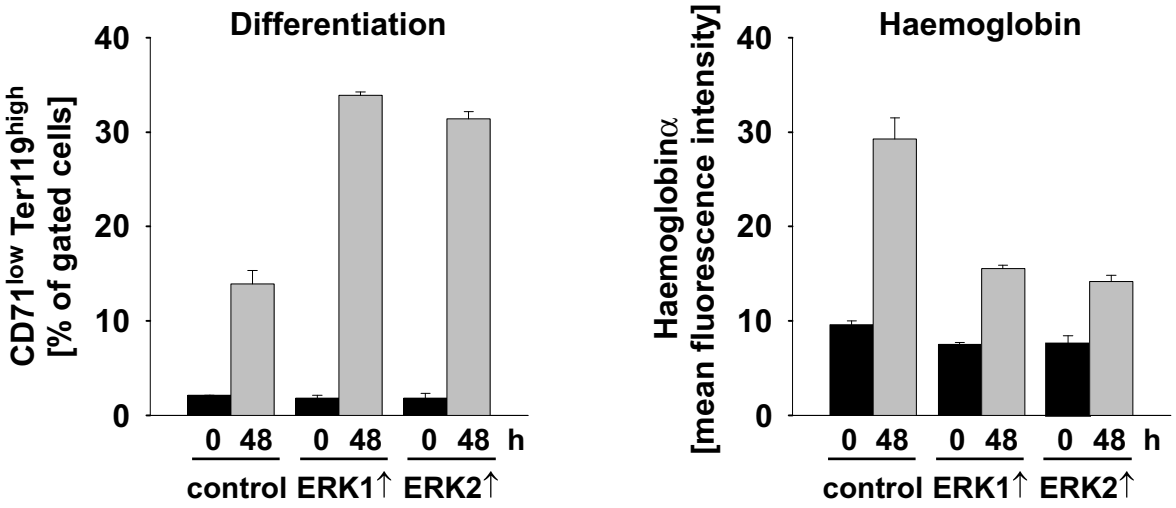

Supplementary Figure 14, Schilling, Maiwald et al.